Effect of external magnetic and electric fields and strains on diamond with negatively charged nitrogen vacancies

A. A. Zvyagin[1,2,3] and G. A. Zvyagina[1]
[1]*B. Verkin Institute for Low Temperature Physics and Engineering of the National Academy of Sciences of Ukraine, Nauky Ave., 47, 61103 Kharkiv, Ukraine*
[2]*Max-Planck-Institut für Physik komplexer Systeme, Nöthnitzer Strasse, 38, D-01187 Dresden, Germany*
[3]*V. N. Karazin Kharkiv National University, Svobody Sq., 4, 61002 Kharkiv, Ukraine*

(Received 19 January 2025; revised 3 April 2025; accepted 19 May 2025; published 3 June 2025)

Characteristics of magneto-electro-elastic effects in a diamond with negatively charged nitrogen vacancy centers are calculated analytically. It is predicted that strains or the external electric field can cause the onset of projections of the magnetic moment of those vacancies perpendicular to the applied magnetic field. It is shown how spins of those vacancies produce the anisotropy of the electric permittivity of a diamond, which depends on the external magnetic field and temperature. The temperature- and magnetic-field-dependent renormalization of elastic modules of a diamond caused by spin quadrupole moments of negatively charged nitrogen vacancy centers is calculated. The predicted effects can be important in the practical use of diamond nanocrystals with color vacancies as local sensors in modern nanoelectroncs.

DOI: 10.1103/PhysRevB.111.214406

I. INTRODUCTION

Magnetic anisotropy is a generic property of magnetic systems [1]. Despite its relativistic origin, it can drastically change the properties of magnetic media [2]. For instance, in magnetically ordered systems the magnetic anisotropy causes such known phenomena as metamagnetism, spin-flop transitions, weak ferromagnetism, and so on [3]. One of the possible realizations of quantum multilevel magnetic systems with an anisotropy are paramagnets. Unlike magnetically ordered systems, the properties of which can be described by classical approaches [1], the magnetic properties of single magnetic ions directly reveal the quantum nature of magnetism since they are related to the discrete spectra of those ions [4,5]. The anisotropic properties of single magnetic ions are caused by the common effect of the crystalline electric field of ligands (nonmagnetic ions, which surround the magnetic ion) and the spin-orbit interaction. The crystalline electric field and the spin-orbit coupling lift the degeneracy of the energy levels of the term of the magnetic ion, resulting in splitting into several multiplets. As a rule, the magnetic anisotropy of paramagnetic ions is manifested in effective g-factors and in the onset of spin (for transition-metal ions) or total moment (for rare-earth ions) multipole operators in the Hamiltonian. The latter exist only for values of spins or total moments of the localized electrons larger than or equal to 1. The important feature of quadrupole moments is their linear coupling to the external electric field [6] or strains [7].

The magnetic anisotropy can exist not only for commonly known magnetic ions with not totally filled $3d$ or $4f$ cells of localized electrons. One of the best studied during the last decades examples of systems, for which the magnetic anisotropy plays a crucial role, are nitrogen vacancy centers in a diamond, see, e.g., the review articles [8–11]. Color centers in a diamond are defects, like vacancies (missing atoms), impurities, or combinations of both. They can change the optical properties of a diamond crystal due to impurity or vacancy levels situated within the excitation gap of a diamond. Transitions between those levels yield optical excitations, which cause sharp zero photon lines in the visible light spectrum. As a result, those defects are the reason for a color of otherwise transparent diamond crystals. Color centers in a diamond are promising subjects as single-photon emitters for applications in sensing [12], quantum computing [13], and even in quantum cryptography [14].

Detection (sensing) of magnetic fields is the principally important problem in many areas of science, computing, technology, and medicine. Sensors based on various techniques have been developed, see, e.g., [15–17]. Nitrogen vacancies in a diamond as sensors have the advantage of high sensitivity detection with nanoscale resolution when using diamond nanocrystals [18,19]. Nitrogen vacancies in a diamond are used for detecting dc and ac magnetic fields [20–24], for which the small size of diamond nanocrystals and long coherence times [25] are beneficial. The detection of ac magnetic fields produced by magnetic moments at nanoscales have interesting applications in magnetic resonance technique, where existing methods for detecting ac magnetic fields use the microwave frequency. Also, optical magnetic resonances use combinations of microwave and optical frequencies [26–28]. For both cases the magnetic anisotropy of negatively charged nitrogen vacancies plays a crucial role, producing the zero-field splitting of spin levels [29–32]. Detection of the dc

magnetic field and slow time-varying one using negatively charged nitrogen vacancies in a diamond have been also studied [33–39]. It is often important to measure not only the magnitudes, but also the directions of magnetic fields caused by magnetic excitations and current distributions in magnetic systems, and negatively charged nitrogen vacancy centers are also used for that purpose [40]. Last but not least, negatively charged nitrogen vacancy centers are used as sensors for the electric field [41] and strain [42].

In this paper we analytically calculate how the interaction between spin degrees of freedom of negatively charged nitrogen vacancies in a diamond and external electromagnetic fields and strains manifests themselves. Namely, we show that the external electric field and strains can cause the reduction of the local symmetry of the vacancy, which, in turn, produces the onset of magnetic moments perpendicular to the direction of the applied magnetic field. We also show that the interaction of spin quadrupole moments of the considered nitrogen vacancies with the electric field causes the onset of the anisotropy of the electric permittivity of the diamond. Finally, the magnetic-field and temperature dependencies of the elastic modules of a diamond, caused by the interaction with spin degrees of freedom of negatively charged nitrogen vacancies are calculated. In our study we do not consider the effect of the hyperfine coupling between the moments of electrons and those of nuclei of the negatively charged nitrogen vacancy. Since the parameters of the hyperfine interaction are of order of 10^{-4} K [43,44], our results can be applied for diamond nanocrystals with negatively charged nitrogen vacancy centers in the temperature range above that value. For the same reason we can neglect the interaction between spins of negatively charged vacancy centers. The main interaction between spins of such vacancies is believed to be of the magnetic dipole-dipole origin. For the considered system it is expected to be of order of 10^{-3} K for a vacancy separation distance of 1.5 nm [45]. Notice, however, that the anisotropy of the magnetic dipole-dipole interaction can itself produce the reduction of the magnetic anisotropy of spins of negatively charged nitrogen vacancies down to triclinic one, which can cause the onset of magnetic moments perpendicular to the direction of the applied magnetic field as well. The model considered in this paper treats the lattice strain as an externally imposed parameter, independent of temperature. It can be reasonable at low temperatures, studied in our work, since they are much smaller than the Debye temperature of a diamond (∼1900 K). Our results can be very important for the application of diamond nanocrystals with negatively charged nitrogen vacancies since they show how even small changes of strains and external electric fields can affect, in a qualitative way, the magnetic response of the system. On the other hand, we show how the magnetic field can change the elastic and electric characteristics of diamond nanocrystals with negatively charged nitrogen vacancies.

II. THEORETICAL FRAMEWORK

If the negatively charged nitrogen vacancy is present in a diamond, then the operator of the energy of its spin subsystem can be written as the contributions from the crystalline electric field and the Zeeman term caused by the external magnetic field **H**. Since the vacancy axis is directed parallel to the [111] diagonal of the cubic cell of the diamond with the local symmetry of ligands (nonmagnetic ions surrounding the magnetic vacancy) being C_{3v}, and the spin of the lowest-energy term $^3A_2$ of the negatively charged nitrogen vacancy is $S = 1$, the Hamiltonian of the spin subsystem of the vacancy is

$$\mathcal{H}_s = DO_2^0 - \hat{g}\mu_B \mathbf{H}\cdot\mathbf{S}, \tag{1}$$

where D is the crystalline electric field of ligands, $O_2^0 = S_z^2 - 2/3 \equiv S_z^2 - S(S+1)/3$ is the Stevens equivalent operator (here we use not the traditional notation of the Stevens operator [46], but rather the one used for the negatively charged nitrogen vacancies, see, e.g., [10], similar to [47]), where $S_{x,y,z}$ are the operators of the projections of the spin 1, $\hat{g}$ is the g-tensor, and μ_B is Bohr's magneton. Here the axis z is chosen to be directed along the [111] axis of the crystal for convenience.

The Hamiltonian of the coupling of the elastic subsystem with the spin one can be written as [48]

$$\begin{aligned}\mathcal{H}_{se} = {} & [h_{41}(\epsilon_{xx}+\epsilon_{yy}) + h_{43}\epsilon_{zz}]O_2^0 \\ & + \left[h_{26}\epsilon_{zx} - \frac{h_{25}}{2}(\epsilon_{xx}-\epsilon_{yy})\right]O_2^1 \\ & + [h_{26}\epsilon_{yz} + h_{25}\epsilon_{xy}]\Omega_2^1 \\ & - \frac{1}{2}\left[h_{16}\epsilon_{zx} - \frac{h_{15}}{2}(\epsilon_{xx}-\epsilon_{yy})\right]O_2^2 \\ & - \frac{1}{4}[h_{16}\epsilon_{yz} + h_{15}\epsilon_{xy}]\Omega_2^2,\end{aligned} \tag{2}$$

where h_{ij} are coupling constants and

$$\begin{aligned} O_2^1 &= \frac{1}{4}[S_zS_+ + S_+S_z + S_zS_- + S_-S_z], \\ \Omega_2^1 &= \frac{1}{4i}[S_zS_+ + S_+S_z - S_zS_- - S_-S_z], \\ O_2^2 &= \frac{1}{2}[S_+^2 + S_-^2], \quad \Omega_2^2 = \frac{1}{2i}[S_+^2 - S_-^2] \end{aligned} \tag{3}$$

are Stevens equivalent operators with $S_\pm = S_x \pm iS_y$. The three basis vectors in the coordinate frame related to the nitrogen vacancy can be chosen, e.g., as $e_x = (1,1,2)/\sqrt{6}$, $e_y = (1,1,0)/\sqrt{2}$, and $e_z = (1,1,1)/\sqrt{3}$ [49].

III. RESULTS

A. Effect of strains on magnetic moments of negatively charged nitrogen vacancies

The calculations of the expectation values of the operators of spin projections, quadrupole operators, and their derivatives (susceptibilities) are presented in Appendix A. Here we show those results in the figures, which illustrate the main features of the temperature and magnetic-field behavior of a negatively charged nitrogen vacancy center in a diamond caused by the coupling of the center to strains.

In Figs. 1 and 2 we present the behavior of the expectation values of the projections of the spin of the negatively charged nitrogen vacancy $S_{x,z}^e \equiv M_{x,z}/g_{x,z}\mu_B$, $M_{x,z}$ are the projections of the magnetic moment of that vacancy center as functions

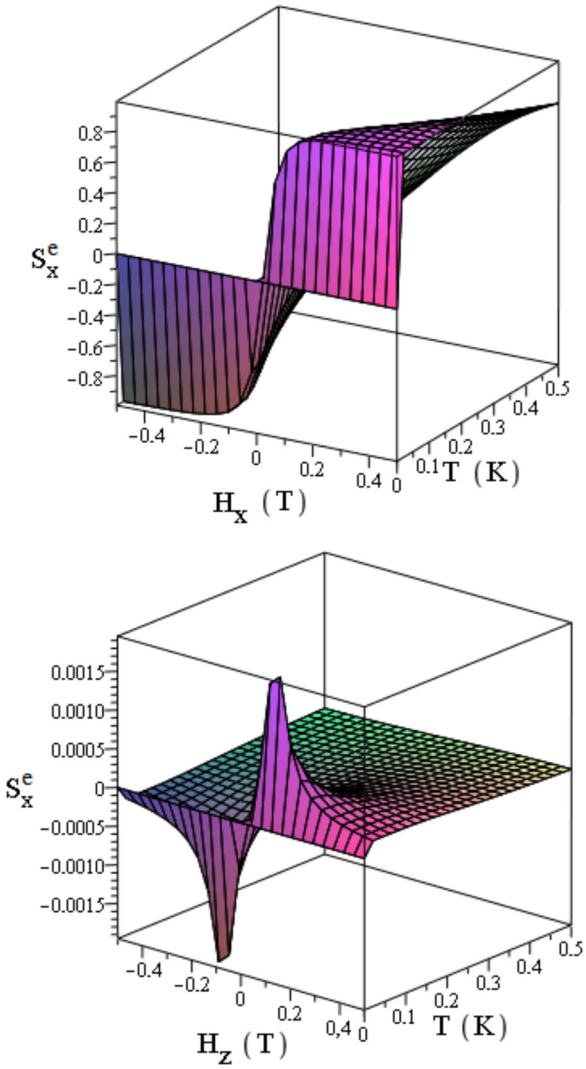

FIG. 1. Upper panel: The dependence of the x-projection of the spin moment of the negatively charged nitrogen vacancy in a diamond due to strains as a function of the external magnetic field H_x and temperature per impurity. Lower panel: The same for the magnetic field H_z.

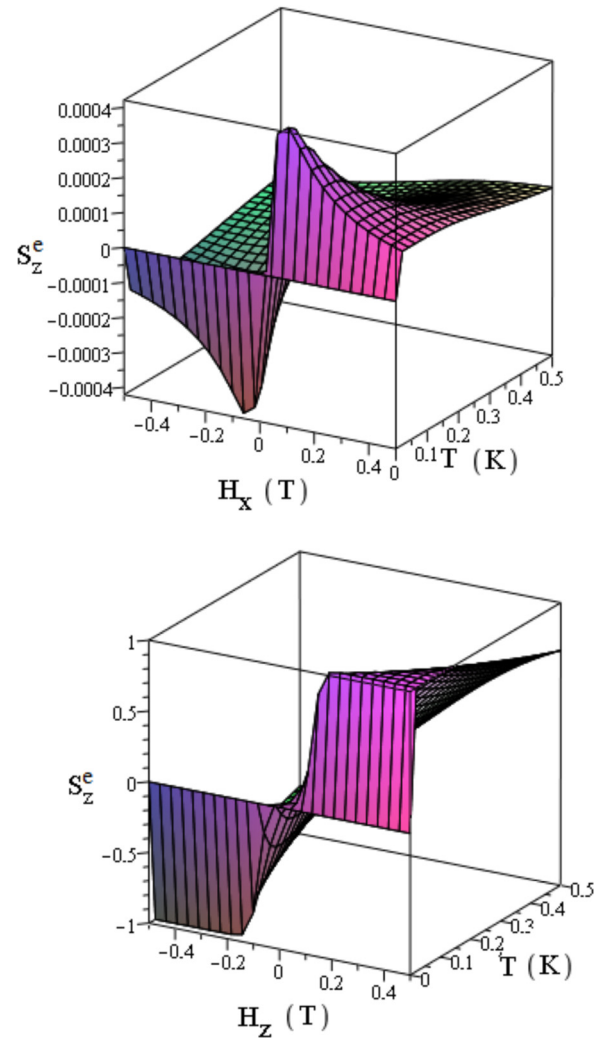

FIG. 2. Upper panel: The dependence of the z-projection of the spin moment of the negatively charged nitrogen vacancy in a diamond due to the strains as a function of the external magnetic field H_x and temperature per impurity. Lower panel: The same for the magnetic field H_z.

of the temperature and the external magnetic fields H_x and H_z obtained with the Gibbs distribution as a function of the temperature and the external magnetic fields. The behavior of M_y is qualitatively similar to M_x. One can see from the figures that the values $S^e_{x,z}$ as a rule decrease with the growth of the temperature at large enough T.

One can see from Fig. 1 that the H_x dependence of S^e_x is smooth, the expectation value of the spin projection grows with the increase of the applied magnetic field. It is nonzero at any value of H_x (even in the ground state), and it reaches almost nominal value (1) at the field value $g_x\mu_B H_x \sim D$. On the other hand, surprisingly, the nonzero (though small) value of S^e_z appears for $H_z = 0$, however, for $H_x \neq 0$. It first increases with the growth of H_x, reaches maximum, and then decreases with H_x as it is further increased. It is the consequence of the onset of the term O^1_2 in the Hamiltonian, i.e., the triclinic symmetry C_1 caused by the strains of the diamond lattice.

We can see from Fig. 2 a similar behavior of S^e_z. The main difference with S_x is the plateau at small values of H_z (for $g_z\mu_B H_z < D$, which is related to the singlet ground state for the easy-plane-like magnetic anisotropy of the vacancy spin $D > 0$), though the temperature of order of D "smears out" that plateau. Nonzero value of S^e_z for $H_z = 0$ and $H_x \neq 0$ is caused by the effective crystalline electric field b^1_2 due to strains.

Notice that, in the absence of the reduction of the symmetry for the negatively charged nitrogen vacancy center (i.e., in the case of the C_{3v} symmetry), S^e_z in Fig. 1 and S^e_x in Fig. 2 are equal to zero for any values of the temperature and magnetic fields H_x and H_z, respectively.

For our calculations we use the values for the coupling constants h_{ij} obtained from the density functional theory [48] ($h_{41} = -0.308$ K/strain; $h_{43} = 0.110$ K/strain; $h_{15} = 0.274$ K/strain; $h_{16} = -0.943$ K/strain; $h_{25} = -0.125$ K/strain; $h_{26} = -0.136$ K/strain) and the strain values 0.001 [50],

so that $b_2^0 = 0.13743$ K ($D = 0.1377$ K [9]) and so on. The results of the estimations [48] are similar to the observations in a diamond with negatively charged vacancy centers [10].

According to the electron spin resonance data [51–53] the components of the g-factors of the negatively charged nitrogen vacancy are equal $g_x = g_y = g_z = 2.0028(3)$ (while the other study reports $g_x = g_y = 2.0031(2)$ and $g_z = 2.0029(2)$ [54]). Hence $g_{x,y,z}$ for the negatively charged nitrogen vacancy are shifted by very small values $\sim 10^{-4}$ from the free electron g-factor $g_e = 2.0023$, i.e., the contribution from the orbital moment is small. From the figures we see the crossover at values of the $H_z \sim b_2^0$ for the magnetic field parallel to the [111] axis, while for the magnetic field directed perpendicular to [111] the crossover exists only at $H_{x,y} = 0$.

We check that, for the original crystalline electric field $D \neq 0$ and $b_2^{1,2} = c_2^{1,2} = 0$, i.e., in the absence of strains, the negatively charged nitrogen vacancy manifests the standard behavior: $M_{x,y,z} \neq 0$ only in the respected nonzero values of $H_{x,y,z}$ (i.e., the magnetic moment is caused only by the parallel applied magnetic field).

We also calculated the expectation values of the components of the spin quadrupole moment $Q_2^{0,1,2} = \langle O_2^{0,1,2} \rangle$ and $q_2^{1,2} = \langle \Omega_2^{1,2} \rangle$. Except for Q_2^0 and Q_2^2 the other components of the spin quadrupole moment are small because they are caused by small strains. The temperature dependence manifests the nonmonotonic changes at low temperatures, and then a decay of the expectation values of the components of the spin quadrupole moment with the growth of T. Also, the expectation values of the components of the spin quadrupole moment are even functions of the applied magnetic field $H_{x,y,z}$. As a rule they decay with the growth of the value of the magnetic field, except for Q_2^2, which shows a nonmonotonic behavior with the growth of $H_{x,y}$.

Hence, strains of the crystal lattice of a diamond cause the very interesting phenomenon, the onset of the nonzero values of the expectation values of the magnetic moment in the magnetic fields directed *perpendicular* to the direction of the magnetic moment. Such a phenomenon is caused by the triclinic distortions of ligands surrounding the spin of the negatively charged nitrogen vacancy.

B. Effect of the electric field

Similar results were obtained for the magnetic-field behavior of magnetic moments of negatively charged nitrogen vacancy centers under the action of the external electric field. The electric field acts on the spin of the vacancy as [48]

$$\mathcal{H}_{es} = d_\parallel E_z O_2^0 + 2d'_\perp \left[E_x O_2^1 + E_y \Omega_2^1\right] + d_\perp \left[-E_x O_2^2 + \frac{E_y}{2} \Omega_2^2\right], \tag{4}$$

where $E_{x,y,z}$ are the projections of the external electric field, and $d_\parallel$, $d_\perp$, and $d'_\perp$ are the spin-electric coupling parameters. It means that the electric field can produce effects similar to strains, i.e., the onset of nonzero projection of the magnetic moment in magnetic fields directed perpendicular to the spin projection. Notice, however, that for the negatively charged nitrogen vacancies the values $d_\parallel \sim 0.168 \times 10^{-6}$ K cm/V, $d_\perp \sim 8 \times 10^{-6}$ K cm/V, and $d'_\perp \sim 0$ [41,55] (some sources imply $d'_\perp \sim d_\perp$ [48]) are smaller than h_{ij} [48], and, hence the effect of the electric field is expected to be weaker than the one of strains for negatively charged nitrogen vacancies in diamond.

C. Effect of the magnetic field on elastic modules

Then, let us consider the elastic subsystem of a diamond. The elastic energy for the cubic symmetry of the diamond lattice per volume can be written as

$$E_{el} = \tfrac{1}{2}\left[C_{11}\left(\epsilon_1^2 + \epsilon_2^2 + \epsilon_3^2\right) + C_{44}\left(\epsilon_4^2 + \epsilon_5^2 + \epsilon_6^2\right)\right] + 2C_{12}(\epsilon_1\epsilon_2 + \epsilon_1\epsilon_3 + \epsilon_2\epsilon_3), \tag{5}$$

where we use the Voight notations for indices $i = 1, \ldots, 6$, with $1 = XX$, $2 = YY$, $3 = ZZ$, $4 = XZ$, $5 = YZ$, $6 = XY$ symmetric with respect to all pair permutations, i.e., e.g., $XY = YX$ and so on (capital letters denote coordinates related to the diamond cubic lattice), ϵ_i are the strains, and C_{ij} are the elastic modules.

It is possible to connect the strains in coordinates related to the negatively charged nitrogen vacancy center with the ones, related to the coordinates of the diamond lattice

$$\begin{aligned}
\epsilon_{xx} + \epsilon_{yy} + \epsilon_{zz} &= \epsilon_1 + \epsilon_2 + \epsilon_3 = \epsilon_b,\\
2\epsilon_{zz} - \epsilon_{xx} - \epsilon_{yy} &= 2(\epsilon_5 + \epsilon_4 + \epsilon_6),\\
\epsilon_{zx} &= \frac{1}{3\sqrt{2}}(2\epsilon_3 - \epsilon_1 - \epsilon_2) - \frac{1}{3\sqrt{2}}(2\epsilon_6 - \epsilon_4 - \epsilon_5),\\
\epsilon_{yz} &= \frac{1}{\sqrt{6}}(\epsilon_1 - \epsilon_2) + \frac{1}{\sqrt{6}}(\epsilon_5 - \epsilon_4),\\
\epsilon_{xx} - \epsilon_{yy} &= \frac{1}{3}(2\epsilon_3 - \epsilon_1 - \epsilon_2) + \frac{2}{3}(2\epsilon_6 - \epsilon_4 - \epsilon_5),\\
\epsilon_{xy} &= \frac{1}{2\sqrt{3}}(\epsilon_1 - \epsilon_2) - \frac{1}{\sqrt{3}}(\epsilon_5 - \epsilon_4),
\end{aligned} \tag{6}$$

where ϵ_b is the bulk strain.

Let us, for simplicity, consider only deformations of the diamond lattice in the plane including both [001] and [110] axes. For such deformations we have $\epsilon_1 = \epsilon_2$ and $\epsilon_4 = \epsilon_5$. We can also skip the bulk strain ϵ_b, getting

$$\begin{aligned}
\epsilon_{xx} + \epsilon_{yy} &= -\frac{2}{3}(2\epsilon_4 + \epsilon_6),\\
\epsilon_{zz} &= \frac{2}{3}(2\epsilon_4 + \epsilon_6),\\
\epsilon_{zx} &= \frac{2}{3\sqrt{2}}(\epsilon_3 - \epsilon_1) - \frac{2}{3\sqrt{2}}(\epsilon_6 - \epsilon_4),\\
\epsilon_{yz} &= 0, \quad \epsilon_{xy} = 0,\\
\epsilon_{xx} - \epsilon_{yy} &= \frac{2}{3}(\epsilon_3 - \epsilon_1) + \frac{4}{3}(\epsilon_6 - \epsilon_4).
\end{aligned} \tag{7}$$

For that case we can rewrite the Hamiltonian of the spin-elastic coupling as

$$\begin{aligned}\mathcal{H}_{se} = {} & (2\epsilon_4+\epsilon_6)\frac{2}{3}(h_{43}-h_{41})O_2^0 \\ & + \left[(\epsilon_3-\epsilon_1)\left(\frac{\sqrt{2}h_{26}}{3}-\frac{h_{25}}{3\sqrt{2}}\right)\right. \\ & \left. -(\epsilon_6-\epsilon_4)\left(\frac{h_{26}}{3\sqrt{2}}+\frac{4h_{25}}{3}\right)\right]O_2^1 \\ & - \left[(\epsilon_3-\epsilon_1)\left(\frac{h_{16}}{3\sqrt{2}}-\frac{h_{15}}{6}\right)\right. \\ & \left. -(\epsilon_6-\epsilon_4)\left(\frac{h_{16}}{3\sqrt{2}}+\frac{h_{15}}{3}\right)\right]O_2^2. \end{aligned} \tag{8}$$

Using those expressions it is possible to calculate the changes of the elastic modules of a diamond caused by the negatively charged nitrogen vacancies. One can see that namely the elastic modules C_{11}, C_{33}, C_{12}, C_{44}, and C_{66} get renormalized due to the coupling with the spin of the negatively charged nitrogen vacancy. In particular, it is clear that, in the considered case, the elastic modulus C_{22} becomes different from C_{11} and C_{33}, also the elastic modulus C_{44} becomes different from C_{66}.

In acoustic experiments one usually measures the changes of the velocity of sound v, which in highly symmetric crystals is proportional to the elastic modulus as $\rho v^2 = C$, where ρ is the density of the crystal, and C is the elastic modulus. For the cubic system the relevant for our case velocities of sound are the longitudinal ones (with the polarization of the sound wave parallel to its wave vector), namely, the one spreading parallel to the [001] axis of the crystal (related to the change of the elastic modulus C_{33}, and the one spreading parallel to the [110] axis [related to the change of the combination of the elastic modules $C_\perp = (1/2)(C_{11}+C_{12}+2C_{44})$]. Also for our case, the important sound wave is the perpendicular one (with the polarization of the wave perpendicular to the wave vector), spreading along the [001] axis, which is related to the elastic modulus C_{44} [56]. Following [57] we obtain for relevant modules

$$\begin{aligned}\Delta C_{11} = \Delta C_{33} = & -\left(\frac{\sqrt{2}h_{26}}{3}-\frac{h_{25}}{3\sqrt{2}}\right)^2\chi_2^1 - \left(\frac{h_{16}}{3\sqrt{2}}-\frac{h_{15}}{6}\right)^2\chi_2^2, \\ \Delta C_{44} = & -\frac{4}{3}(h_{43}-h_{41})^2\chi_2^0 - \left(\frac{h_{26}}{3\sqrt{2}}+\frac{4h_{25}}{3}\right)^2\chi_2^1 \\ & - \left(\frac{h_{16}}{3\sqrt{2}}+\frac{h_{15}}{3}\right)^2\chi_2^2, \\ \Delta C_\perp \equiv {} & \frac{1}{2}(\Delta C_{11}+\Delta C_{12}+2\Delta C_{44}) \\ = {} & \frac{1}{4}\Delta C_{11}+\Delta C_{44}, \\ \Delta C_{66} = {} & \Delta C_{44}+\frac{2}{3}(h_{43}-h_{41})^2\chi_2^0, \end{aligned} \tag{9}$$

where $\chi_2^{1,2} = \partial Q_2^{1,2}/\partial b_2^{1,2}$ is the spin quadrupole susceptibility.

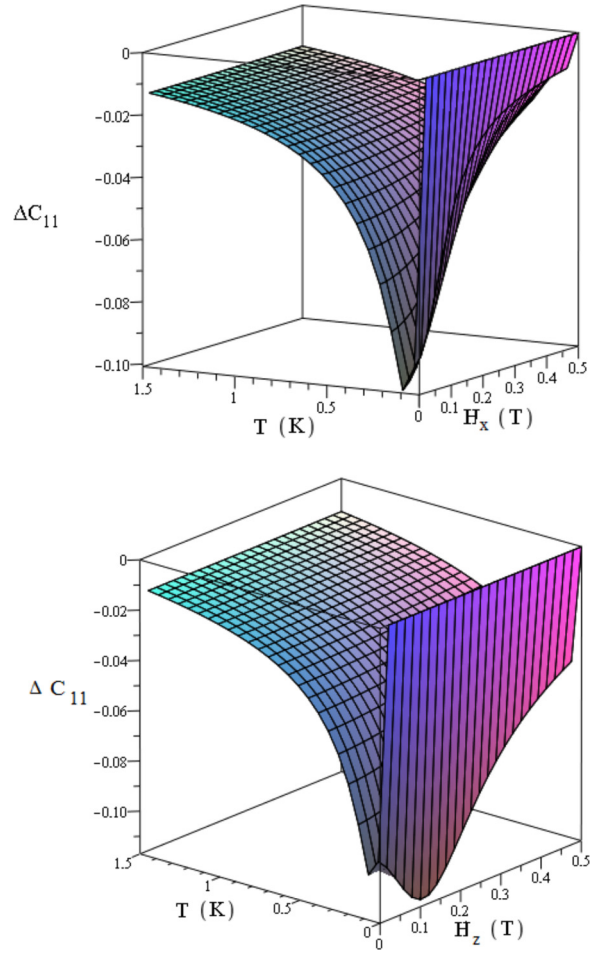

FIG. 3. Upper panel: The dependencies of the changes of the elastic modulus ΔC_{11} (in K/strain^2) of a diamond due to the negatively charged nitrogen vacancy on the external magnetic field H_x and temperature per impurity. Lower panel: The same for the magnetic field H_z.

Figures 3–6 show the results of calculations of the renormalization of elastic modules in a diamond caused by the interaction of strains with the spin of the negatively charged nitrogen vacancy. Notice that the results are present per vacancy, therefore, to get the answer for a nanocrystal (nanocrystals of a diamond are used as sensors) one needs to multiply the presented results by the concentration of negatively charged nitrogen vacancy centers in that diamond nanocrystal.

The results are presented as functions of the temperature and the external magnetic field directed along the z ([111]) axis of the crystal and along the x axis (see above). In the considered case, the difference for the renormalization of the elastic modules in the field H_x and H_y is small.

One can see that the temperature dependence manifests the softening of elastic modules with the decrease of T and hardening at very low temperatures. The magnetic-field dependence also shows the decrease of elastic modules with the decrease of H_x. On the other hand, H_z-dependence manifests the nonmonotonic behavior, with the minimum, which is determined by the value of D. Notice that at

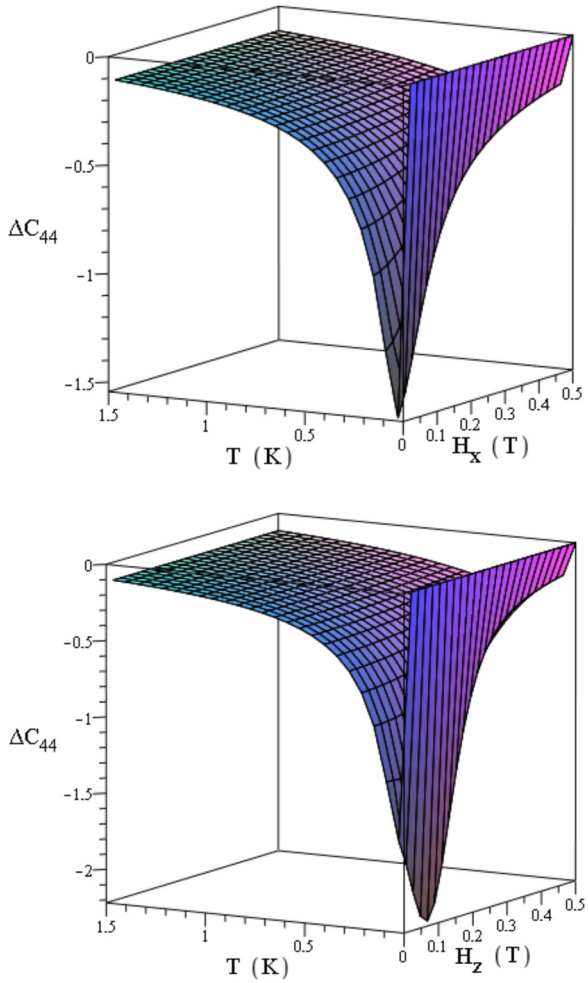

FIG. 4. Upper panel: The dependencies of the changes of the elastic modulus ΔC_{44} (in K/strain^2) of a diamond due to the negatively charged nitrogen vacancy on the external magnetic field H_x and temperature per impurity. Lower panel: The same for the magnetic field H_z.

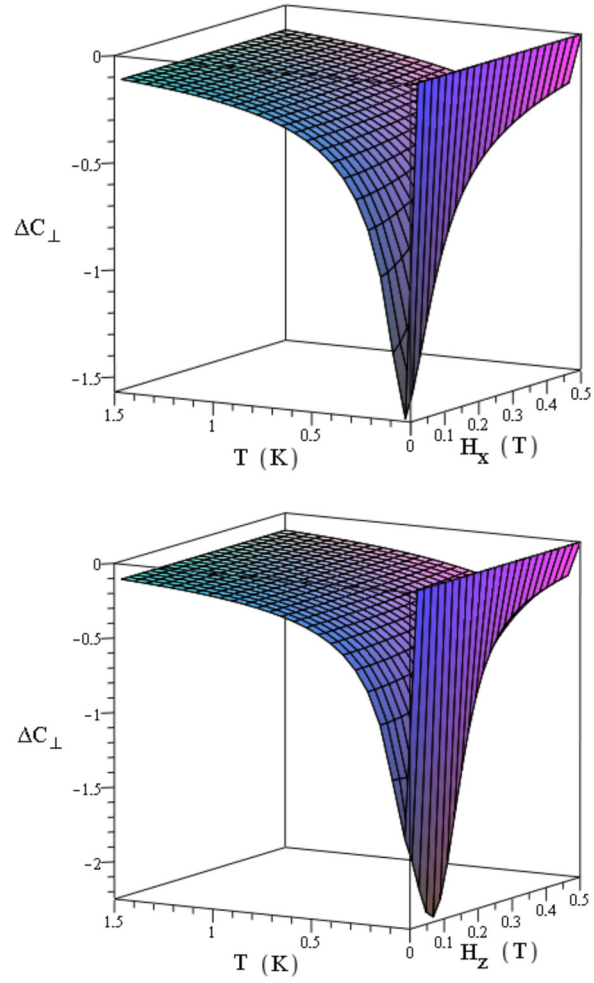

FIG. 5. Upper panel: The dependencies of the changes of the elastic modulus $\Delta C_{\perp}$ (in K/strain^2) of a diamond due to the negatively charged nitrogen vacancy on the external magnetic field H_x and temperature per impurity. Lower panel: The same for the magnetic field H_z.

$g\mu_B H_z = D$ the crossover takes place, at which the magnetic moment manifests jump from zero to $\sim g\mu_B$.

We emphasize that maximal changes are seen for the elastic modules C_{44} and C_{66} (and related $C_{\perp}$), with respect to C_{11} and C_{33}. Notice, however, that, namely, C_{33} and C_{11} manifest low-temperature low-field nonmonotonic dependencies. In experiments, the difference will be seen even more dramatically because, in experiments, one usually measures the relative changes of elastic modules (or associated changes of velocities of sound), $\Delta C/C$, and for diamond C_{44} is of an order of magnitude smaller than C_{11} [48]. The results of the low-temperature low-energy calculations are presented in Appendix B.

D. Renormalization of the electric permittivity

In a similar way [57], we calculated the renormalization of the electric permittivity of a diamond caused by the negatively charged nitrogen vacancies. That effect is also proportional to the concentration of such vacancies, i.e., it will be more manifested in diamond nanocrystals. The effective values of the electric permittivity $\varepsilon_{x,y,z}$ are determined from the Hamiltonians $\mathcal{H}_s + \mathcal{H}_{es}$ together with the Hamiltonian of the electric field

$$\mathcal{H}_e = -\sum_{j=x,y,z} \frac{\varepsilon_j E_j^2}{\varepsilon_0}, \tag{10}$$

where ε_0 is the vacuum permittivity. We obtain

$$\begin{aligned} \varepsilon_x^{\text{eff}} &= \varepsilon_x + (2d'_{\perp})^2 \chi_2^1 + d_{\perp}^2 \chi_2^2, \\ \varepsilon_y^{\text{eff}} &= \varepsilon_y + (2d'_{\perp})^2 (\chi')_2^1 + 4d_{\perp}^2 (\chi')_2^2, \\ \varepsilon_z^{\text{eff}} &= \varepsilon_z + d_{\parallel}^2 \chi_2^0, \end{aligned} \tag{11}$$

where $(\chi')_2^{1,2} = \partial q_2^{1,2}/\partial c_2^{1,2}$ are the quadrupole susceptibilities related to spin quadrupole moments $\Omega_2^{1,2}$. Notice that for the cubic symmetry $\varepsilon_x = \varepsilon_y = \varepsilon_z = \varepsilon$ [1], ε is equal to 5.7 for a diamond [41]. It is clear from these expressions that the renormalization of the electric permittivity of a diamond caused by negatively charged nitrogen vacancies is small, however, it produces the difference between three components of the tensor of electric permittivity. Since the

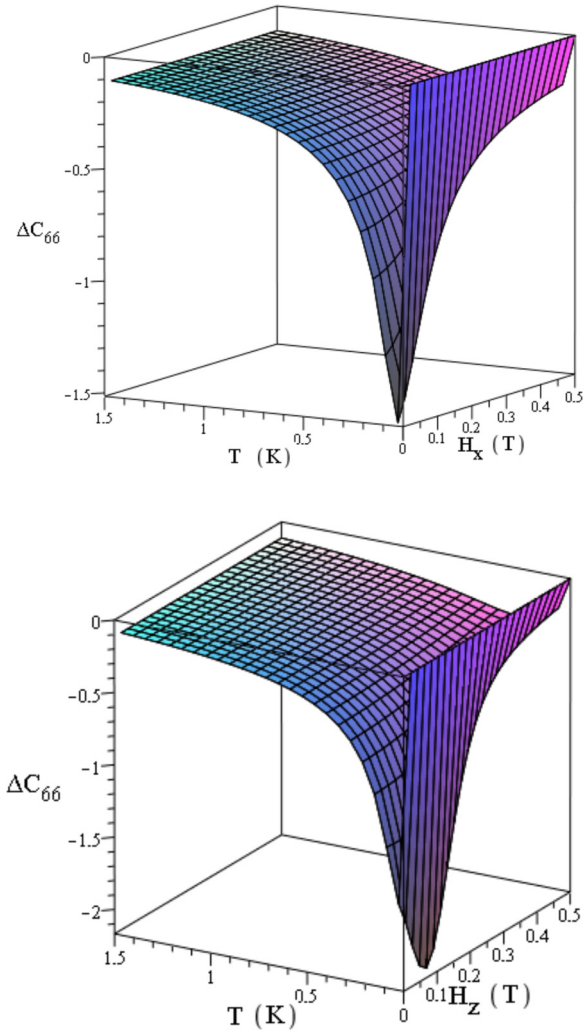

FIG. 6. Upper panel: The dependencies of the changes of the elastic modulus ΔC_{66} (in K/strain^2) of a diamond due to the negatively charged nitrogen vacancy on the external magnetic field H_x and temperature per impurity. Lower panel: The same for the magnetic field H_z.

renormalization of the components of the tensor of the electric permittivity (11) is determined by the components of the spin quadrupole susceptibility as the renormalization of elastic modules (9) (with the opposite sign, though), the temperature and magnetic-field dependencies of the correction to the electric permittivity will be similar to the ones presented in Figs. 3–6 (however, with different sign and scales).

IV. SUMMARY

In summary, we analytically calculated several characteristics of magneto-electro-elastic effects in a diamond with negatively charged nitrogen vacancies. The reason for those effects is the coupling of the spin degrees of freedom of those vacancies with the electric field and strains. Predicted effects are proportional to the concentration of vacancies, which can be large enough in nanocrystals. The qualitative effect of negatively charged nitrogen vacancy centers in diamond is the magnetic-field dependence of elastic modules. In a pure diamond (without mentioned vacancies), the elastic modules, obviously, do not depend on the external magnetic field. Since we do not study the interaction between negatively charged nitrogen vacancy centers, the predicted effects are linearly proportional to the concentration of the latter. Also there are four possible orientations for the studied vacancy axis in the diamond lattice. Naturally, the effect for the general case has to be proportional to 1/4 of the concentration of negatively charged nitrogen vacancy centers. Notice, however, that it is possible to utilize diamond nanocrystals with a fixed orientation of the negatively charged nitrogen vacancy axis [58].

In particular, we showed that strains or the external electric field can cause an interesting effect: the onset of projections of the magnetic moment of vacancies perpendicular to the applied magnetic field. Since strains can be very small, and nanocrystals of a diamond with negatively charged nitrogen vacancies are suggested as sensors for local magnetic and electric fields and strains, the predicted effect can be very important when determining the values of magnetic moments for studied subjects, e.g., in electron spin resonance and optical magnetic resonance experiments. Also, we showed how the spin quadrupole moments of the vacancies renormalize the electric permittivity of a diamond resulting in the anisotropy of the latter. That anisotropy depends on the external magnetic field and temperature. Finally, we calculated how spin quadrupole moments of nitrogen vacancy centers renormalize elastic modules of a diamond as a function of the magnetic field and temperature. We predicted the most drastic changes of elastic modules, and, hence, sound velocities, for transverse modules and sound waves. Our results show how even small changes of strains and external electric fields affect the magnetic response, and how the magnetic field can change the elastic and electric characteristics of diamond nanocrystals with magnetic vacancies. This is why that influence has to be taken into account for precise determination of local magnetic, electric, and elastic characteristics of subjects, which can be measured using such diamond nanocrystals as sensors. Since diamond nanocrystals with magnetic vacancies are commonly believed to be used as local sensors in many nanodevices, including quantum computers, the predicted effects can be very important in spintronics and nanotechnology.

ACKNOWLEDGMENTS

A.A.Z. acknowledges the support from the Deutsche Forschugsgemeinschaft via the SFB 1143. G.A.Z. acknowledges the support from the Wolfgang Pauli Institut within the WPI thematic program "Numerical Modelling of Quantum Experiments" (2024/2025).

DATA AVAILABILITY

No data were created or analyzed in this study.

APPENDIX A: CALCULATIONS OF THE ENERGIES

In this Appendix we present the way of calculation of magnetic and quadrupole characteristics of the triclinic paramagnet $S = 1$. Let us write the Hamiltonian

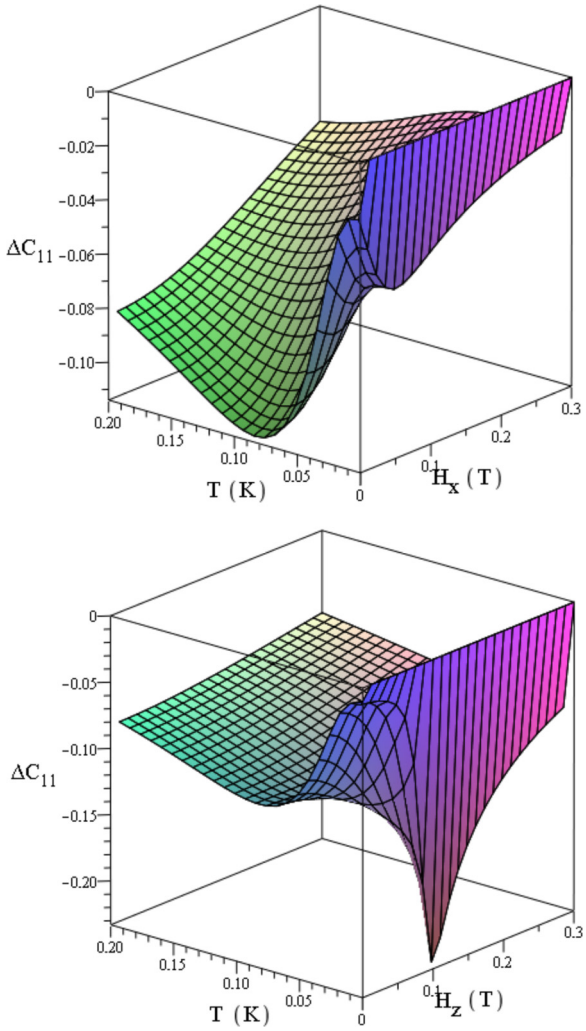

FIG. 7. Upper panel: The low-temperature low-field dependencies of the changes of the elastic modulus ΔC_{11} (in K/strain^2) of a diamond due to the negatively charged nitrogen vacancy on the external magnetic field H_x and temperature per impurity. Lower panel: The same for the magnetic field H_z.

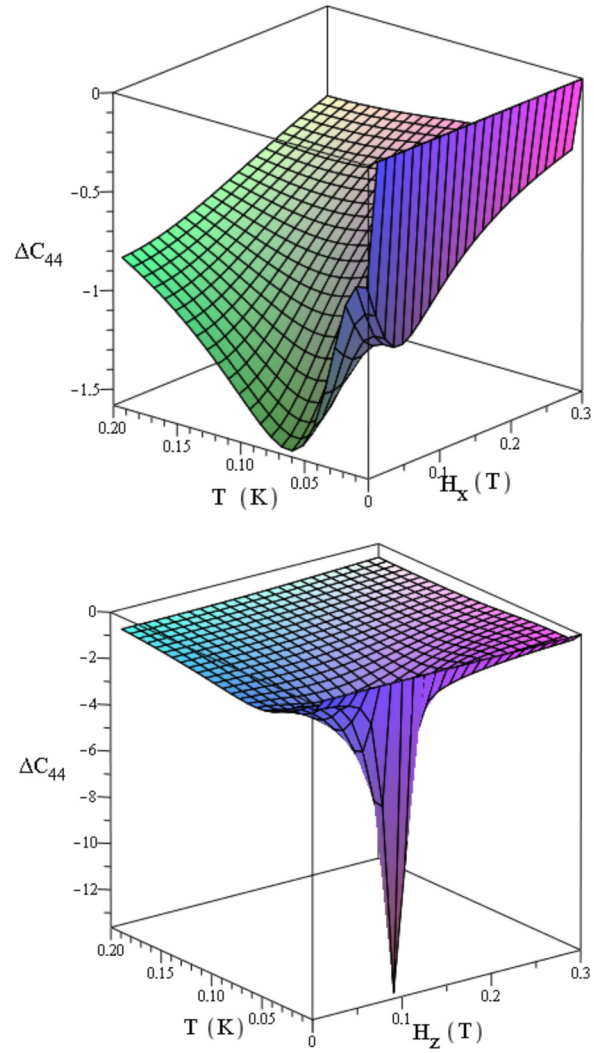

FIG. 8. Upper panel: The low-temperature low-field dependencies of the changes of the elastic modulus ΔC_{44} (in K/strain^2) of a diamond due to the negatively charged nitrogen vacancy on the external magnetic field H_x and temperature per impurity. Lower panel: The same for the magnetic field H_z.

of the system as

$$\mathcal{H} = \sum_{n=0}^{2} \left(b_2^n O_2^n + c_2^n \Omega_2^n\right) - \mu_B \sum_{i=x,y,z} g_i H_i S_i, \tag{A1}$$

where b_2^m and c_2^m are standard notation for the crystalline electric fields [46,47]. Then the eigenvalues of the Hamiltonian (A1) are

$$\begin{aligned} \varepsilon_1 &= u + v, \\ \varepsilon_{2,3} &= -\frac{u+v}{2} \pm i\sqrt{3}\frac{u-v}{2}, \end{aligned} \tag{A2}$$

where

$$\begin{aligned} u &= \left(-\frac{q}{2} + \sqrt{d}\right)^{1/3}, \\ v &= \left(-\frac{q}{2} - \sqrt{d}\right)^{1/3}, \\ d &= \left(\frac{p}{3}\right)^3 + \left(\frac{q}{2}\right)^2, \end{aligned}$$

$$\begin{aligned} p &= \frac{3s - r^2}{3}, \\ q &= \frac{27t + 2r^3 - sr}{27}. \end{aligned} \tag{A3}$$

Here we denote

$$\begin{aligned} s &= \left(b_2^0\right)^2 - \left(b_2^1/2\right)^2 - \left(b_2^2\right)^2 - \left(c_2^1/2\right)^2 - \left(c_2^2\right)^2 \\ &\quad - (g_x\mu_B H_x)^2 - (g_y\mu_B H_y)^2 - (g_z\mu_B H_z)^2, \\ t &= b_2^0\left[\left(b_2^1/2\right)^2 + \left(c_2^1/2\right)^2 + (g_x\mu_B H_x)^2 + (g_y\mu_B H_y)^2\right] \\ &\quad - g_z\mu_B H_z\left[b_2^1 g_x\mu_B H_x + c_2^1 g_y\mu_B H_y\right] \\ &\quad + b_2^2\left[\left(b_2^1/2\right)^2 - \left(c_2^1/2\right)^2 - (g_x\mu_B H_x)^2 + (g_y\mu_B H_y)^2\right] \\ &\quad + \left(c_2^2/2\right)\left[b_2^1 c_2^1 - 4 g_x g_y \mu_B^2 H_x H_y\right], \\ r &= -2b_2^0. \end{aligned} \tag{A4}$$

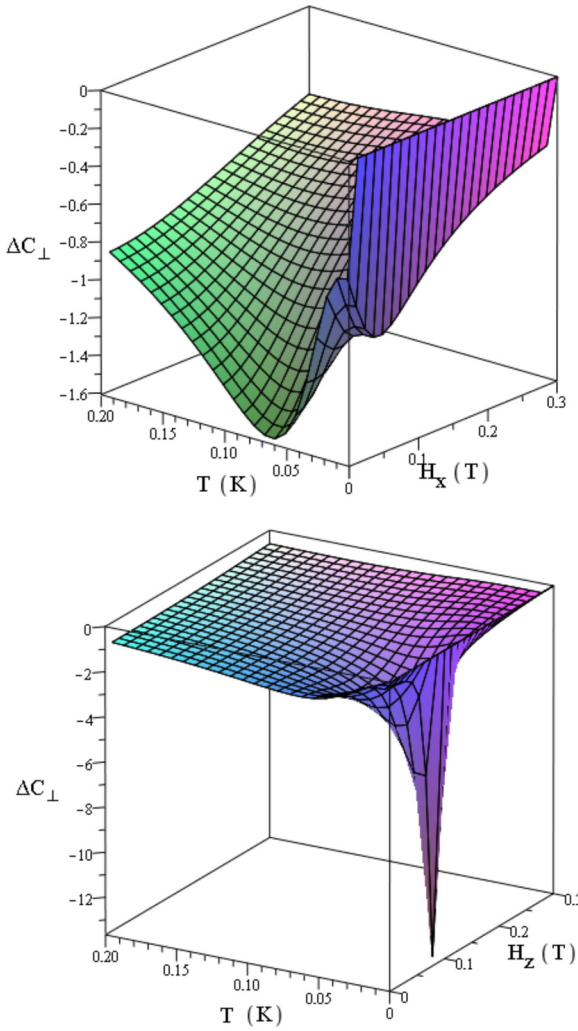

FIG. 9. Upper panel: The low-temperature low-field dependencies of the changes of the elastic modulus $\Delta C_\perp$ (in K/strain^2) of a diamond due to the negatively charged nitrogen vacancy on the external magnetic field H_x and temperature per impurity. Lower panel: The same for the magnetic field H_z.

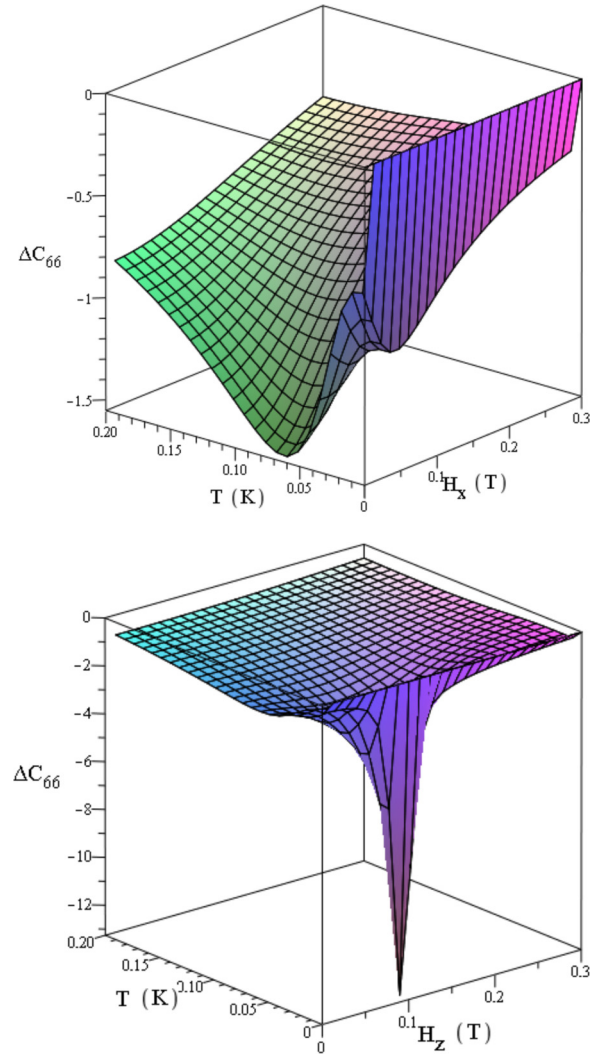

FIG. 10. Upper panel: The low-temperature low-field dependencies of the changes of the elastic modulus ΔC_{66} (in K/strain^2) of a diamond due to the negatively charged nitrogen vacancy on the external magnetic field H_x and temperature per impurity. Lower panel: The same for the magnetic field H_z.

Then, as usually the partition function of the spin is $Z = \sum_{i=1}^{3} \exp(-\varepsilon_i/k_BT)$, where k_B is the Boltzmann constant, T is the temperature, and the free energy is $f = -k_BT\ln(Z)$. The calculations of the expectation values of the operators of projections of the spin, and quadrupole moments and their derivatives are then obvious, however, the analytic results are too long (more than several pages of formulas) to be presented in the paper. Effective crystalline fields which appear due to all possible strains acting on the negatively charged nitrogen vacancy in a diamond are related to connection of the Hamiltonians (A1) and $\mathcal{H}_s + \mathcal{H}_{se}$. Namely, we use $b_2^0 = D + h_{41}(\epsilon_{xx} + \epsilon_{yy}) + h_{43}\epsilon_{zz}$, $b_2^1 = h_{26}\epsilon_{zx} - (h_{25}/2)(\epsilon_{xx} - \epsilon_{yy})$, $b_2^2 = -(1/2)[h_{16}\epsilon_{zx} - (h_{15}/2)(\epsilon_{xx} - \epsilon_{yy})]$, $c_2^1 = h_{26}\epsilon_{yz} + h_{25}\epsilon_{xy}$, and $c_2^2 = -(1/4)[h_{16}\epsilon_{yz} + h_{15}\epsilon_{xy}]$.

APPENDIX B: RESULTS FOR THE LOW-ENERGY BEHAVIOR

In this Appendix we present the results of low-temperature low-field calculations for the changes of elastic modules of a diamond with negatively charged nitrogen vacancy. The results are shown in Figs. 7–10 for the external magnetic field directed along the z ([111]) axis of the crystal, and along the x axis (see above). In the considered case the difference for the renormalization of the elastic modules in the field H_x and H_y is also small.

The results are shown per negatively charged nitrogen vacancy. To get the result for a nanocrystal (namely, nanocrystals of a diamond are used as sensors in many cases) one needs to multiply the presented results by the concentration of negatively charged nitrogen vacancy centers in that diamond nanocrystal.

One can see a very different behavior of elastic modules for the magnetic field directed along the [111] axis, and perpendicular to that axis. For the former we can see the pronounced minimum of the renormalized elastic modules at zero temperature at the field value determined by the crystalline

electric field value D. On the other hand, for the magnetic field perpendicular to the [111] axis, minimal values of the renormalizations of elastic modules is seen at zero field value at temperatures about 0.1 K.

[1] L. D. Landau and E. M. Lifshitz, *Electrodynamics of Continuous Media* (Pergamon, Oxford, 1984).

[2] A. A. Zvyagin, *Quantum Theory of One-Dimensional Spin Systems* (Cambridge Scientific Publishers, Cambridge, England, 2010).

[3] R. M. White, *Quantum Theory of Magnetism* (Springer, New York, 1983).

[4] W. Low, *Paramagnetic Resonance in Solids*, Solid State Physics V. 2, Supplement (Academic Press, New York, 1960).

[5] M. Tinkham, *Group Theory and Quantum Mechanics* (McGraw-Hill, New York, 1964).

[6] N. Bloembergen, Linear Stark effect in magnetic resonance spectra, Science **133**, 1363 (1961).

[7] B. Lüthi, *Physical Acoustics in the Solid State* (Springer, Berlin, 2005).

[8] F. Jelezko and J. Wrachtrup, Single defect centres in diamond: A review, Phys. Status Solidi (a) **203**, 3207 (2006).

[9] M. W. Doherty, N. B. Manson, P. Delaney, F. Jelezko, J. Wrachtrup, and L. C. L. Hollenberg, The nitrogen-vacancy colour centre in diamond, Phys. Rep. **528**, 1 (2013).

[10] R. Schirhagl, K. Chang, M. Loretz, and C. L. Degen, Nitrogen-vacancy centers in diamond: Nanoscale sensors for physics and biology, Annu. Rev. Phys. Chem. **65**, 83 (2014).

[11] J. F. Barry, J. M. Schloss, E. Bauch, M. I. Turner, C. A. Hart, L. M. Pham, and R. L. Walsworth, Sensitivity optimization for NV-diamond magnetometry, Rev. Mod. Phys. **92**, 015004 (2020).

[12] J. Hruby, M. Gulka, M. Mongillo, I. P. Radu, M. V. Petrov, E. Bourgeois, and M. Nesladek, Magnetic field sensitivity of the photoelectrically read nitrogen-vacancy centers in diamond, Appl. Phys. Lett. **120**, 162402 (2022).

[13] F. Jelezko, T. Gaebel, I. Popa, M. Domhan, A. Gruber, and J. Wrachtrup, Observation of coherent oscillation of a single nuclear spin and realization of a two-qubit conditional quantum gate, Phys. Rev. Lett. **93**, 130501 (2004).

[14] N. Gisin, G. Ribordy, W. Tittel, and H. Zbinden, Quantum cryptography, Rev. Mod. Phys. **74**, 145 (2002).

[15] D. Budker and M. Romalis, Optical magnetometry, Nat. Phys. **3**, 227 (2007).

[16] R. L. Fagaly, Superconducting quantum interference device instruments and applications, Rev. Sci. Instrum. **77**, 101101 (2006).

[17] M. Vengalattore, J. M. Higbie, S. R. Leslie, J. Guzman, L. E. Sadler, and D. M. Stamper-Kurn, High-resolution magnetometry with a spinor Bose-Einstein condensate, Phys. Rev. Lett. **98**, 200801 (2007).

[18] S. Hong, M. S. Grinolds, L. M. Pham, D. L. Sage, L. Luan, R. L. Walsworth, and A. Yacoby, Nanoscale magnetometry with NV centers in diamond, MRS Bull. **38**, 155 (2013).

[19] L. Rondin, J.-P. Tetienne, T. Hingant, J.-F. Roch, P. Maletinsky, and V. Jacques, Magnetometry with nitrogen-vacancy defects in diamond, Rep. Prog. Phys. **77**, 056503 (2014).

[20] C. L. Degen, Scanning magnetic field microscope with a diamond single-spin sensor, Appl. Phys. Lett. **92**, 243111 (2008).

[21] J. R. Maze, P. L. Stanwix, J. S. Hodges, S. Hong, J. M. Taylor, P. Cappellaro, L. Jiang, M. V. G. Dutt, E. Togan, A. S. Zibrov, A. Yacoby, R. L. Walsworth, and M. D. Lukin, Nanoscale magnetic sensing with an individual electronic spin in diamond, Nature (London) **455**, 644 (2008).

[22] P. Appel, M. Ganzhorn, E. Neu, and P. Maletinsky, Nanoscale microwave imaging with a single electron spin in diamond, New J. Phys. **17**, 112001 (2015).

[23] S. Schmitt, T. Gefen, F. M. Stürner, T. Unden, G. Wolff, C. Müller, J. Scheuer, B. Naydenov, M. Markham, S. Pezzagna, J. Meijer, I. Schwarz, M. Plenio, A. Retzker, L. P. McGuinness, and F. Jelezko, Submillihertz magnetic spectroscopy performed with a nanoscale quantum sensor, Science **356**, 832 (2017).

[24] J. Zhang and D. Suter, Single NV centers as sensors for radio-frequency fields, Phys. Rev. Res. **5**, L022026 (2023).

[25] J. M. Boss, K. S. Cujia, J. Zopes, and C. L. Degen, Quantum sensing with arbitrary frequency resolution, Science **356**, 837 (2017).

[26] F. Bitter, The optical detection of radiofrequency resonance, Phys. Rev. **76**, 833 (1949).

[27] D. Suter, Optical detection of magnetic resonance, Magnetic Resonance **1**, 115 (2020).

[28] A. Dréau, M. Lesik, L. Rondin, P. Spinicelli, O. Arcizet, J.-F. Roch, and V. Jacques, Avoiding power broadening in optically detected magnetic resonance of single nv defects for enhanced dc magnetic field sensitivity, Phys. Rev. B **84**, 195204 (2011).

[29] J. M. Taylor, P. Cappellaro, L. Childress, L. Jiang, D. Budker, P. R. Hemmer, A. Yacoby, R. Walsworth, and M. D. Lukin, High-sensitivity diamond magnetometer with nanoscale resolution, Nat. Phys. **4**, 810 (2008).

[30] K. R. K. Rao and D. Suter, Level anti-crossings of a nitrogen-vacancy center in diamond: decoherence-free subspaces and 3d sensors of microwave magnetic fields, New J. Phys. **22**, 083035 (2020).

[31] P. Wang, Z. Yuan, P. Huang, X. Rong, M. Wang, X. Xu, C. Duan, C. Ju, F. Shi, and J. Du, High-resolution vector microwave magnetometry based on solid-state spins in diamond, Nat. Commun. **6**, 6631 (2015).

[32] G. Wang, Y.-X. Liu, Y. Zhu, and P. Cappellaro, Nanoscale vector ac magnetometry with a single nitrogen-vacancy center in diamond, Nano Lett. **21**, 5143 (2021).

[33] B. J. Maertz, A. P. Wijnheijmer, G. D. Fuchs, M. E. Nowakowski, and D. D. Awschalom, Vector magnetic field microscopy using nitrogen vacancy centers in diamond, Appl. Phys. Lett. **96**, 092504 (2010).

[34] H. Clevenson, L. M. Pham, C. Teale, K. Johnson, D. Englund, and D. Braje, Robust high-dynamic-range vector magnetometry with nitrogen-vacancy centers in diamond, Appl. Phys. Lett. **112**, 252406 (2018).

[35] C. Zhang, H. Yuan, N. Zhang, L. Xu, J. Zhang, B. Li, and J. Fang, Vector magnetometer based on synchronous manipulation of nitrogen-vacancy centers in all crystal directions, J. Phys. D: Appl. Phys. **51**, 155102 (2018).

[36] H. Zheng, Z. Sun, G. Chatzidrosos, C. Zhang, K. Nakamura, H. Sumiya, T. Ohshima, J. Isoya, J. Wrachtrup, A. Wickenbrock,

and D. Budker, Microwave-free vector magnetometry with nitrogen-vacancy centers along a single axis in diamond, Phys. Rev. Appl. **13**, 044023 (2020).

[37] B. Chen, X. Hou, F. Ge, X. Zhang, Y. Ji, H. Li, P. Qian, Y. Wang, N. Xu, and J. Du, Calibration-free vector magnetometry using nitrogen-vacancy center in diamond integrated with optical vortex beam, Nano Lett. **20**, 8267 (2020).

[38] D. A. Broadway, S. E. Lillie, S. C. Scholten, D. Rohner, N. Dontschuk, P. Maletinsky, J.-P. Tetienne, and L. C. L. Hollenberg, Improved current density and magnetization reconstruction through vector magnetic field measurements, Phys. Rev. Appl. **14**, 024076 (2020).

[39] T. Weggler, C. Ganslmayer, F. Frank, T. Eilert, F. Jelezko, and J. Michaelis, Determination of the three-dimensional magnetic field vector orientation with nitrogen vacancy centers in diamond, Nano Lett. **20**, 2980 (2020).

[40] F. Casola, T. van der Sar, and A. Yacoby, Probing condensed matter physics with magnetometry based on nitrogen-vacancy centres in diamond, Nat. Rev. Mater. **3**, 17088 (2018).

[41] F. Dolde, H. Fedder, M. W. Doherty, T. Nöbauer, F. Rempp, G. Balasubramanian, T. Wolf, F. Reinhard, L. C. L. Hollenberg, F. Jelezko, and J. Wrachtrup, Electric-field sensing using single diamond spins, Nat. Phys. **7**, 459 (2011).

[42] M. E. Trusheim and D. Englund, Wide-field strain imaging with preferentially aligned nitrogen-vacancy centers in polycrystalline diamond, New J. Phys. **18**, 123023 (2016).

[43] J. R. Rabeau, R. Reichart, G. Tamanyan, D. N. Jammieson, S. Prawer, F. Jelezko, T. Gaebel, I. Popa, M. Domhan, and J. Wrachtrup, Implantation of labelled single mitrogen vacancy centers in diamond using ^{15}N, Appl. Phys. Lett. **88**, 023113 (2006).

[44] A. Dréau, J.-R. Maze, M. Lesik, J.-F. Roch, and V. Jacques, High resolution spectroscopy of single NV defects coupled with nearby ^{13}C nuclear spins in diamond, Phys. Rev. B **85**, 134107 (2012).

[45] T. Gaebel, M. Domhan, I. Popa, C. Wittmann, P. Neumann, F. Jelezko, J. R. Rabeau, N. Stavrias, A. D. Greentree, S. Prawer, J. Meijer, J. Twamley, P. R. Hemmer, and J. Wrachtrup, Room temperature coherent control of coupled single spins in solid, Nat. Phys. **2**, 408 (2006).

[46] A. Abragam and B. Bleaney, *Electron Paramagnetic Resonance of Transition Ions* (Clarendon, Oxford, 1970).

[47] A. I. Freeman and R. E. Watson, Theoretical investigation of some magnetic and spectroscopic properties of rare-earth ions, Phys. Rev. **127**, 2058 (1962).

[48] P. Udvarhelyi, V. O. Shkolnikov, A. Gali, G. Burkard, and A. Pályi, Spin-strain interaction in nitrogen-vacancy centers in diamond, Phys. Rev. B **98**, 075201 (2018).

[49] M. Koga and M. Matsumoto, Magnetoacoustic resonance to probe quadrupole–strain coupling in a diamond nitrogen-vacancy center as a spin-triplet system, J. Phys. Soc. Jpn. **89**, 113701 (2020).

[50] J. Teissier, A. Barfuss, P. Appel, E. Neu, and P. Maletinsky, Strain coupling of a nitrogen-vacancy center spin to a diamond mechanical oscillator, Phys. Rev. Lett. **113**, 020503 (2014).

[51] J. H. N. Loubser and J. A. van Wyk, Electron spin resonance in the study of diamond, Rep. Prog. Phys. **41**, 1201 (1978).

[52] X.-F. He, N. B. Manson, and P. T. H. Fisk, Paramagnetic resonance of photoexcited N-V defects in diamomd. I. Level anticrossing in the ^3A state, Phys. Rev. B **47**, 8809 (1993).

[53] X.-F. He, N. B. Manson, and P. T. H. Fisk, Paramagnetic resonance of photoexcited N-V defects in diamomd. II. Hyperfine interaction with ^{14}N nucleus, Phys. Rev. B **47**, 8816 (1993).

[54] S. Felton, A. M. Edmonds, M. E. Newton, P. M. Martineau, D. Fisher, D. J. Twitchen, and J. M. Baker, Hyperfine interaction in the groud state of the negatively charged nitrogen vacancy center in diamond, Phys. Rev. B **79**, 075203 (2009).

[55] E. Van Oort and M. Glasbeek, Electric-field induced modulation of spin echoes of N-V centers in diamond, Chem. Phys. Lett. **168**, 529 (1990).

[56] R. Truell, C. Elbaum, and B. B. Chik, *Ultrasonic Methods in Solid State Physics* (Academic, New York, 1969).

[57] A. A. Zvyagin and G. A. Zvyagina, Piezoelectric and magnetoelastic effects in a quantum paramagnet, Fiz. Nizk. Temp. **47**, 140 (2021) [Low Temp. Phys. **47**, 123 (2021)].

[58] K. Ogawa, M. Tsukamoto, Y. Mori, D. Takafuji, J. Shiogai, K. Ueda, J. Matsuno, J.-I. Ohe, K. Sasaki, and K. Kobayashi, Quantitative imaging of nonlinear spin-wave propagation using diamond quantum sensors, arXiv:2503.23321v1.